

# **Turbulent Heat Transfer in Buoyancy-Driven Natural Convection in Vertical Enclosures (Draft)**

Abstract—In this work, turbulent heat transfer in buoyancy-driven natural convection in vertical enclosures is studied numerically by finite element method. A scheme that involves a statistical quantity is applied to detect the onset of the multi-cellular turbulence in rectangular cavities with aspect ratio larger than 30. Below 30, the limit of transition from laminar to single-cellular turbulent flow is found by solving the laminar and turbulent governing equations and comparing the difference of heat transfer results between them. Turbulent flow in enclosures with aspect ratio from 20 to 100 is then modeled for Rayleigh number up to 200,000. And a correlation of average Nusselt number is developed as a function of Rayleigh number and aspect ratio.

## **1. Introduction**

Buoyancy-driven natural convection in confined enclosures is receiving more and more research attention due to its wide applications, such as multi-layered walls, double-pane windows and other air gaps in unventilated spaces. Understanding the physics of flows in confined enclosures can greatly enhance the efficiency of utilization of building systems.

Depending on the conditions such as size and shape of the enclosure and the heating applied, the flows in the enclosure can be either laminar or turbulent. While laminar flow is relatively simple and well defined, turbulent flow represents one of most complicated phenomena in the nature. According to Hinze (1959), “Turbulent fluid motion is an irregular condition of flow in which the various quantities show a random variation with time and space coordinates, so that statistically distinct values can be discerned.” From this classical definition, we can tell that turbulence is time-dependent, as well as it is irregularly random so that statistical methods have to be used to study and analyze the characteristics of turbulence.

In engineering applications, turbulence often displays apparent differences from laminar flows. Comparatively speaking, turbulent flows often lead to higher transport rate of momentum, energy and mass than laminar flows. These features are widely made use

of in energy systems in industry. For example, turbulence enhancers such as ribs are added to cooling systems of turbine blades and microelectronic devices to create more turbulent motions so that the overall heat transfer efficiency can be improved. However, turbulence may also be the adverse condition that people try to avoid. For instance, the enhanced heat transfer efficiency caused by turbulence in building systems usually means that more energy will be transferred between the building and its surroundings, resulting in more energy consumption of the building. For this reason, study of the characteristics of turbulent fluid flow and heat transfer is very important for more efficient utilization of building energy system and this is the motivation of this work.

In this work, transitions from laminar flow to turbulence in confined enclosures were first studied. As a very complex process, there have been quite some researchers working on this topic before. Yang (1988), gave a very good summary of this process. He points out that occurrences of flow bifurcations change the structure of the flow and gradually lead to the commencement of turbulence with the change of controlling parameter such as heating. As the underlying mechanism for transition to turbulence is very complicated and the description of this process needs a deep understanding of physics and mathematics, which is not available to most of the designers in engineering field, the first purpose of this paper is to present a correlation of the limit of transition to turbulence with respect to the controlling parameters of the flow. Then, the characteristics of turbulent flow and heat transfer in the enclosures were studied. A simple correlation of heat transfer with respect to the controlling parameters, such as Rayleigh number and aspect ratio, will be given in the turbulent regime. These correlation equations would be easily understandable by designers and applicable as a guide in their design of building systems or other systems where flows in confined enclosures exist.

## **2. Literature review**

Numerous studies can be found in literature on turbulent flow. Several work provided correlations of transitional limit from laminar to turbulent regime in vertical rectangular enclosures. The earliest work can be found in Batchelor (1954). Yin et al (1978) presented measurement data that fluctuated at sufficiently high Ra, and Wright (1990) interpreted this as an indicator of the transition to turbulence. Power (1999) used a

transient method in order to observe any fluctuations of the numerical solution of average Nusselt number over time. Although these three studies all provide simple power law form of correlation for the Rayleigh number limit of transition as a function of aspect ratio, their results lack universal consistency. And the applicable aspect ratio ranges of the given correlations are not large enough and needs to be extended to higher aspect ratio.

Turbulent heat transfer in vertical rectangular enclosures has also been extensively studied by both experimental and numerical work. The early experimental study of Jakob (1967) gave a correlation equation of the form

$$Nu = C(Ra)^a (A)^b \quad (1)$$

with the exponents  $a=1/3$ , and  $b=1/9$  for turbulent flow in cavities with aspect ratio from 3.0 to 42.2. Yin et al (1978) presented a correlation equation with  $a=0.269$  and  $b=0.131$  and the aspect ratio range covers up to 78.7. The experimental work of Elsherbiny et al (1982) provided a set of correlations with more complicated form at aspect ratio  $A=5, 10, 20, 40, 80$  and  $110$ . Raithby and Wong (1981) numerically gave a single but more complicated form of correlation covering aspect ratio from 2 to 80, but with only half of the range of Rayleigh numbers in the current study, which is up to 200,000. More recently, Power (1999) numerically calculated the turbulent heat transfer in cavities with aspect ratios from 5 to 60, and presented correlations of Nusselt number at each aspect ratio that was studied.

Generally speaking, data on turbulent heat transfer in high aspect ratio cavities are scarce. Correlations of turbulent heat transfer presented in literature are mostly only applicable to cavities with low and medium aspect ratio. Even though there are some data available for high aspect ratio cavity flow, such as those of Elsherbiny et al (1982), Yin et al (1978) and Power (1999), the Rayleigh number in their studies only extended slightly beyond the limit of transition to turbulent regime for those cavities with high aspect ratios. In these studies, as aspect ratio increases, the Rayleigh number range being studied narrows.

### 3. Problem description

A two-dimensional rectangular enclosure is shown in Fig. 1. In real application, the enclosure is always three-dimensional. However, the size of the enclosure in the third dimension is usually very big compared to that of the direction with applied temperature gradient. More importantly, there are seldom any effects such as temperature gradient or gravity applied in the third direction, which makes the flow in this direction very close to homogeneous. Thus, in the description of this problem, the third direction is normally neglected.

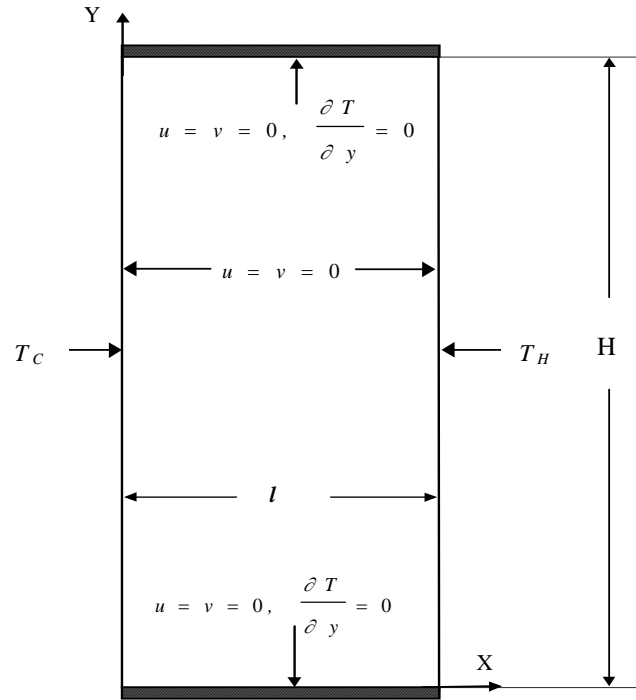


**Figure 1: Confined Rectangular Enclosure Geometry**

From Fig. 1, it can be seen that the two-dimensional enclosure has two horizontal sides and two vertical sides. The two horizontal sides are adiabatic and the two vertical walls have constant temperatures with  $T_H > T_C$ . In this condition, the density gradient of internal fluid is normal to the gravity and natural convection starts immediately when heat is applied.

For calculation purposes, it is often convenient to non-dimensionalize the governing equations and to introduce the characteristic dimensionless numbers. The governing equations are non-dimensionalized based on the following relations and scaling quantities:

$$u^* = \frac{u}{U}, \quad v^* = \frac{v}{U}, \quad U = \frac{\alpha}{L} \sqrt{Ra Pr} = \sqrt{g \beta \Delta T L} \quad (2)$$

$$x^* = \frac{x}{L}, \quad y^* = \frac{y}{L} \quad (3)$$

$$\theta^* = \frac{T - T_0}{\Delta T}, \quad \Delta T = T_H - T_C \quad (4)$$

$$p^* = \frac{pL}{\mu U} \quad (5)$$

$$Ra = \frac{\rho g \beta (T_H - T_C) L^3}{\mu \alpha}, \quad Pr = \frac{\nu}{\alpha} = \frac{\mu C_p}{k} \quad (6)$$

$$t^* = \frac{tU}{L} \quad (7)$$

The Boussinesq approximation, as well as the assumption of an incompressible fluid flow, is applied. The Governing equations in non-dimensional form are:

Continuity equation:  $\frac{\partial u^*}{\partial x^*} + \frac{\partial v^*}{\partial y^*} = 0.$  (8)

Momentum equations:

x-direction:

$$\sqrt{\frac{Ra}{Pr}} \left[ \frac{\partial u^*}{\partial t^*} + u^* \frac{\partial u^*}{\partial x^*} + v^* \frac{\partial u^*}{\partial y^*} \right] = - \frac{\partial p^*}{\partial x^*} + \left[ \frac{\partial^2 u^*}{\partial x^{*2}} + \frac{\partial^2 u^*}{\partial y^{*2}} \right]. \quad (9)$$

y-direction:

$$\sqrt{\frac{Ra}{Pr}} \left[ \frac{\partial v^*}{\partial t^*} + u^* \frac{\partial v^*}{\partial x^*} + v^* \frac{\partial v^*}{\partial y^*} \right] = - \frac{\partial p^*}{\partial y^*} + \left[ \frac{\partial^2 v^*}{\partial x^{*2}} + \frac{\partial^2 v^*}{\partial y^{*2}} \right] + \sqrt{\frac{Ra}{Pr}} \theta^*. \quad (10)$$

Energy equation:

$$\sqrt{Ra Pr} \left[ \frac{\partial \theta^*}{\partial t^*} + u^* \frac{\partial \theta^*}{\partial x^*} + v^* \frac{\partial \theta^*}{\partial y^*} \right] = \frac{\partial^2 \theta^*}{\partial x^{*2}} + \frac{\partial^2 \theta^*}{\partial y^{*2}}. \quad (11)$$

The boundary conditions imposed in the dimensionless form for this problem are as follows:

Temperature boundary conditions on the side walls:

$$\theta^*(x^* = 0, y^*) = 0, \quad \theta^*(x^* = 1, y^*) = 1. \quad (12)$$

Non-slip velocity boundary conditions on all bounding surfaces are:

$$u^*(x^* = 0, y^*) = v^*(x^* = 0, y^*) = 0, \quad (13)$$

$$u^*(x^* = 1, y^*) = v^*(x^* = 1, y^*) = 0, \quad (14)$$

$$u^*(x^*, y^* = 0) = v^*(x^*, y^* = 0) = 0, \quad (15)$$

$$u^*(x^*, y^* = H^*) = v^*(x^*, y^* = H^*) = 0, \quad (16)$$

where  $H^*$  is the dimensionless height of the cavity.

Boundary conditions at the top and bottom surfaces:

$$\text{ZHF: } \left. \frac{\partial \theta^*}{\partial y^*} \right|_{y^*=0} = 0, \quad \left. \frac{\partial \theta^*}{\partial y^*} \right|_{y^*=H^*} = 0. \quad (17)$$

The dimensionless parameters governing the flow behavior in a vertical cavity are, aspect ratio  $A$  and Rayleigh number  $Ra$ . The aspect ratio  $A$  is defined by,

$$A = \frac{H}{L}, \quad (18)$$

where  $H$  is the height of the cavity and  $L$  is the width of the cavity.

Prandtl number ( $Pr$ ) is the property of the fluid, while Rayleigh number ( $Ra$ ) incorporates the influences of fluid property, external thermal boundary condition and domain geometry into a single parameter. Based on the governing equations, it can be seen that  $Ra$  is the main determining parameter in this problem since it represents the driving force in the enclosure – buoyancy, without which there will be no turbulence in the domain. The greater  $Ra$  is, the greater buoyancy effect will be and the flow tends to be more turbulent.

When  $Ra$  is small, which means there is only very weak buoyancy acting on the flow, it can be expected that the flow is laminar, and the convective motion of the flow creates a cell that circulating inside the enclosure. The streamlines of it are presented in Fig. 2a with  $Ra = 5000$ . The aspect ratio of this cavity is 15.

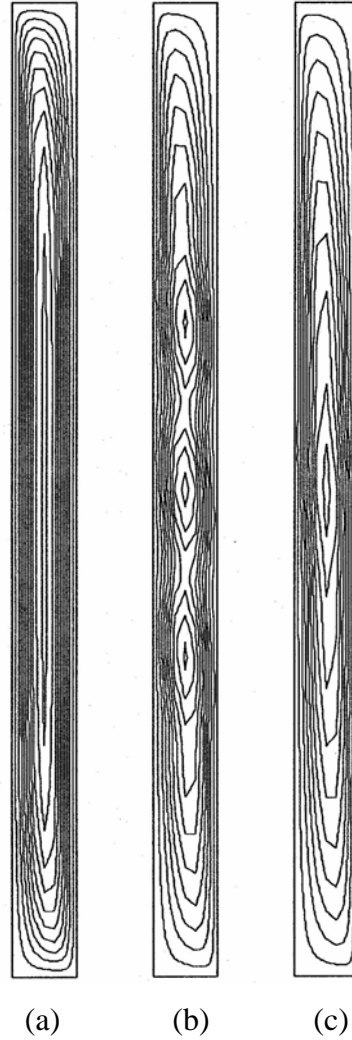


**Figure 2: Cells in a Buoyancy-driven Cavity**

As  $Ra$  increases, an important phenomenon for buoyancy driven cavity flow, multi-cellular condition, will occur, as shown in Fig. 2b. The  $Ra$  under this condition is 17750. There have been intensive investigations on this topic. Batchelor (1954) used linear hydrodynamic stability theory to explain the origin and characteristics of this phenomenon. Zhao (1997), subsequently, applied numerical methods to predict the transitional  $Ra$  between single-cellular and multi-cellular condition with respect to aspect ratio  $A$  in the cavity described as above.

Although the flow in the cavity can become multi-cellular, this condition cannot stay forever for aspect ratio below 30. When the buoyancy force is further strengthened all the small cells will collapse into a single strong cell again. This is the ending point of multi-

cellular regime and was presented by Zhao (1997). The streamlines of this condition are shown in Fig. 2c with  $Ra = 28750$ .

In this research, the derived equation of the limit of transition from laminar flow to turbulence will be the form of Rayleigh number versus aspect ratio, because  $Ra$  is the driving force of the flow and aspect ratio  $A$  is also an important factor that decides the characteristics of the flow. Meanwhile, as both  $Ra$  and  $A$  influence the characteristics of turbulent heat transfer, the overall heat transfer coefficient will be a function in terms of  $Ra$  and  $A$ .

#### **4. Numerical methods**

To solve the problem described by equations 8-11 and boundary conditions 12-17, the finite element analysis method based on the Galerkin weighted residual method is applied. Penalty function method is also used, which utilizes a fluid incompressibility constraint, leading to a reduction of the number of unknowns by eliminating the pressure from the calculations.

In calculations of transition from laminar flow to turbulence, it is a natural choice to use time dependent scheme to solve the problem to discern the temporal fluctuations in the solutions. For calculations in the turbulent regime, time dependent method is also applied to help the convergence of computation. For each enclosure with a specific aspect ratio, the principal controlling parameter,  $Ra$ , is increased incrementally to study the influence of  $Ra$  on heat transfer so that transitional point can be detected and characteristics of heat transfer can be studied. Every new calculation with different Rayleigh number and aspect ratio is initialized using the same initial condition – zero velocity and zero temperature.

A  $k-\omega$  model was used when turbulence model was required. Here,  $k$  represents the turbulent kinetic energy and  $\omega$  is the specific dissipation rate of turbulent kinetic energy. A detailed description of this model can be found in FIDAP (2002).

Nine-node quadratic meshes were generated in the enclosures to perform the computation. The finite-element mesh employed is stretched towards the wall. The mesh density for each aspect ratio is based on the mesh study of Zhao (1997) and Power (1999).



## 5. Transition from laminar to turbulence in vertical enclosures

### 5.1. Principles of detecting transitional points

The most important feature of turbulence is its randomness, and it is assumed that this method can be applied to find the transitional point from laminar flow to turbulence in such a buoyancy-driven cavity. The basic underlying idea is that when the flow goes turbulent, some temporal fluctuations are created in the flow and can be detected numerically by calculating the change of overall heat transfer effect with respect to time so that the flow can be judged to have crossed the transitional limit. It is worth noting here that judging the transitional point using overall heat transfer coefficient is only applicable to flows that cross the transitional point in multi-cellular condition. Due to the instability of the multicells, spatial averaging will not damp out the temporal fluctuation of the overall heat transfer coefficient as the number and location of the cells vary from time to time. On the other hand, when the flow is single-cellular, the overall heat transfer coefficient will not change with respect to time, because spatial averaging can erase all the temporarily fluctuating information.

For this reason, for flows entering turbulent regime in multi-cellular condition, after the time-dependent governing equations are solved, data are collected and overall heat transfer effect with respect to time is computed and recorded to observe the fluctuation. The average Nusselt number (Nu) is defined to quantify the heat transfer effect. Nu has the form as  $Nu = \frac{hL}{k} = \frac{qL}{\Delta Tk}$ , which is the ratio between convection heat transfer to the conduction heat transfer, while q is the overall heat transfer rate. At lower Ra, the Nu is almost a flat line with respect to time, which means there is rarely any fluctuation in the flow. However, as Ra is increased, more fluctuations in Nu can be observed corresponding to the fact that the flow tends to be more turbulent with higher Ra. A good example is given in Fig. 3. A statistical quantity, which is the ratio between the standard deviation and the mean value of Nu over a long range of time, is used to detect the fluctuation.

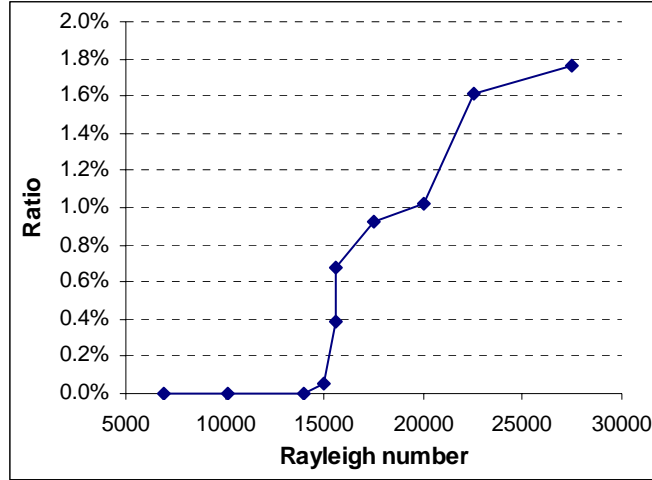


**Figure 3: The Ratio of Standard Deviation to Mean Nusselt Number Vs. Rayleigh Number for Aspect Ratio 40**

It can be seen from Fig. 3 that there is no significant fluctuation at lower range of Rayleigh number. However, as  $Ra$  increases, a sudden increase of fluctuation level can be detected at  $Ra = 16000$ . Further investigation shows that before transition to turbulence, the ratio between standard deviation to the mean value of  $Nu$  is on the order of 0.01% to 0.1%. After it reaches the transitional point, the ratio is at the level of 1%. So the flow can be judged to be turbulent if this ratio reaches 1.0%.

The method above works generally very well for cavities with a wide range of aspect ratios. However, if  $A$  is smaller than 30, the method is very hard to be used to detect the limit of transition. As  $Ra$  is increasing, the flow in the cavity experiences the transition from single-cell to multi-cells. However, it exits multi-cellular condition and returns to single-cell condition before it reaches turbulence regime, according to Zhao (1997). This process can be observed by the variation of the standard deviation of Nusselt number in terms of Rayleigh number. An example for a cavity with  $A=20$  is shown in Fig. 4. In other words, single cell in turbulence regime does not produce discernible fluctuations in average  $Nu$ , so that this method cannot work for cavities with  $A$  below 30.

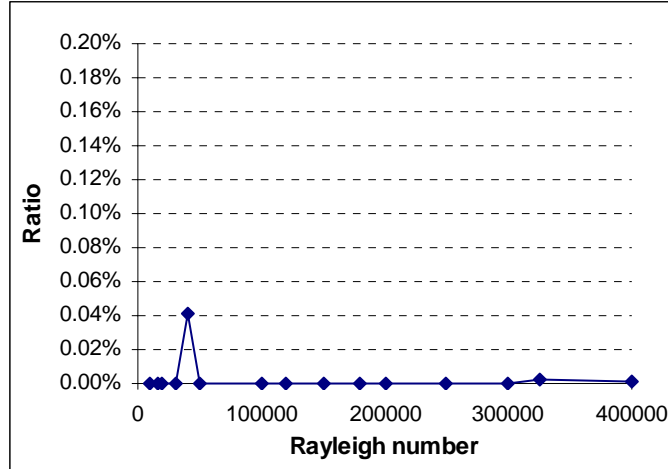


**Figure 4: The Ratio of Standard Deviation to Mean Nusselt Number Vs. Rayleigh Number for Aspect Ratio 20**

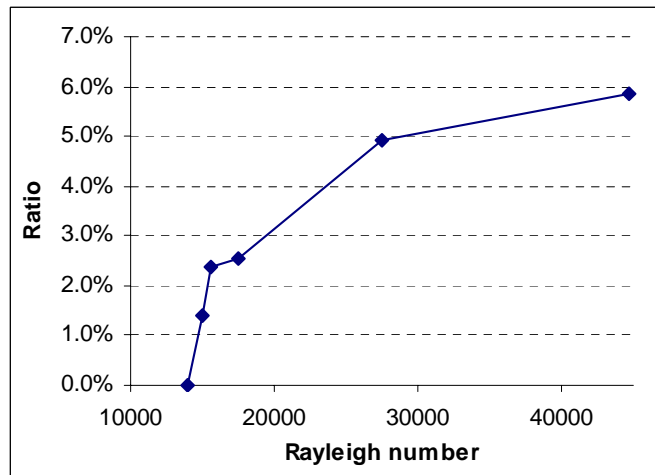


**Figure 5: The Percentage Difference between laminar and turbulent results for aspect ratio 40**

Thus, an alternative method has to be found to detect the onset of turbulence. In this research, two sets of simulations are run to solve for  $Nu$  for each cavity with aspect ratio smaller than at every  $Ra$  it experiences. One simulation is using laminar model while the other one incorporates a  $\kappa-\omega$  turbulence model. Two results are compared and if the difference between each other is larger than 3%, the flow is regarded to be turbulent. The difference is defined as  $(Nu_{tur} - Nu_{lam})/Nu_{tur}$ . The magnitude of the 3 percent difference criterion was determined by comparing Fig. 3 to Fig. 5, which shows the percentage difference between laminar and turbulent results for aspect ratio 40. From Fig. 3, the flow

was judged to be turbulent when Rayleigh number is higher than 20,000, by observing the ratio of the standard deviation to mean Nusselt number reach 1.0%. Then, it is shown from the curve in Fig. 5, that Rayleigh number 20,000 corresponds to 3 percent difference between laminar and turbulent results.

## 5.2. Results and analysis for transition to turbulence

In the range of Rayleigh number covered in this study, the flow remains laminar for enclosures under aspect ratio 20. Thus, the range of aspect ratio starts from 20 and the upper limit is 100.

When  $A$  is larger than 30, the time series of overall heat flux ( $Nu$ ) is recorded and its standard deviation is calculated. For each enclosure, standard deviation of  $Nu$  can be regarded as a function of Rayleigh number. When the ratio between the standard deviation of  $Nu$  and its mean value reaches 1%, the flow is then regarded to have entered the turbulent regime. An example is given in Fig. 3, which shows that for  $A = 40$  flow turns turbulent around  $Ra = 20,000$ .

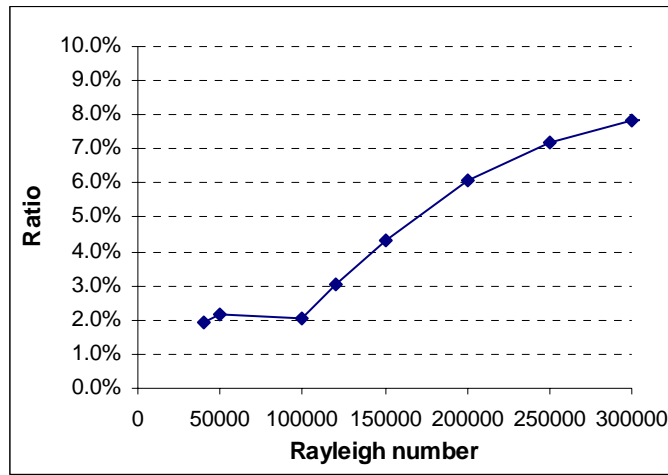


**Figure 6: The Percentage Difference between laminar and turbulent results for aspect ratio 20**

For enclosures with  $A$  smaller than 30, the alternative method, which is to compare the average Nusselt numbers of laminar model and turbulent model, is applied. Whenever the percentage difference of the two results is over 3% of the turbulent value, turbulence is regarded to have occurred in the flow. Such difference for a cavity  $A=20$  is plotted in Fig. 6, and applying the 3 percent criterion gives us a transitional Rayleigh number about 120,000.

The overall results are plotted in Fig. 7, which covers aspect ratios from 20 to 100. For cavities with aspect ratio higher than ???, transitional limit remains a constant value of 21,000??. Batchelor (1954) also predicted that transitional limit became independent of aspect ratio from a critical value of 42, which is very close to the current results, although his constant value of Rayleigh number is 13,700, around 35%?? lower than that of current study.

For aspect ratios less than ??, simulation data from current study produced a simple power law correlation with the form,

$$Ra_c = C(A)^a \quad (19)$$

where  $C = 7 \times 10^8$ ,  $a = -2.8174$ ???. This result is very close to that of Batchelor's with the same form, with coefficient  $C = 10^9$  and exponent  $a = -3$ , as shown in Fig. 7.

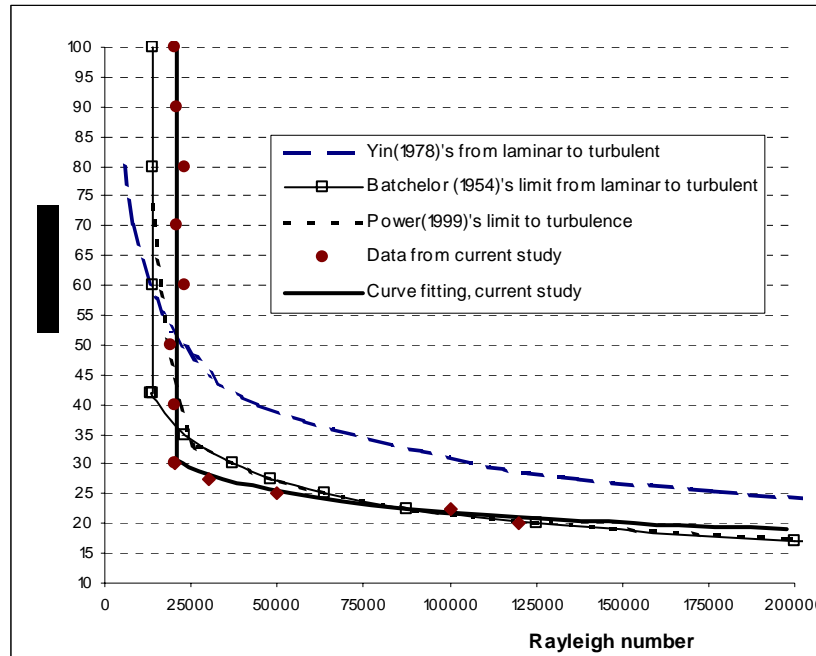


**Figure 7: The Limit of Transition from Laminar to Turbulent Regime**

## 6. Turbulent heat transfer in vertical enclosures

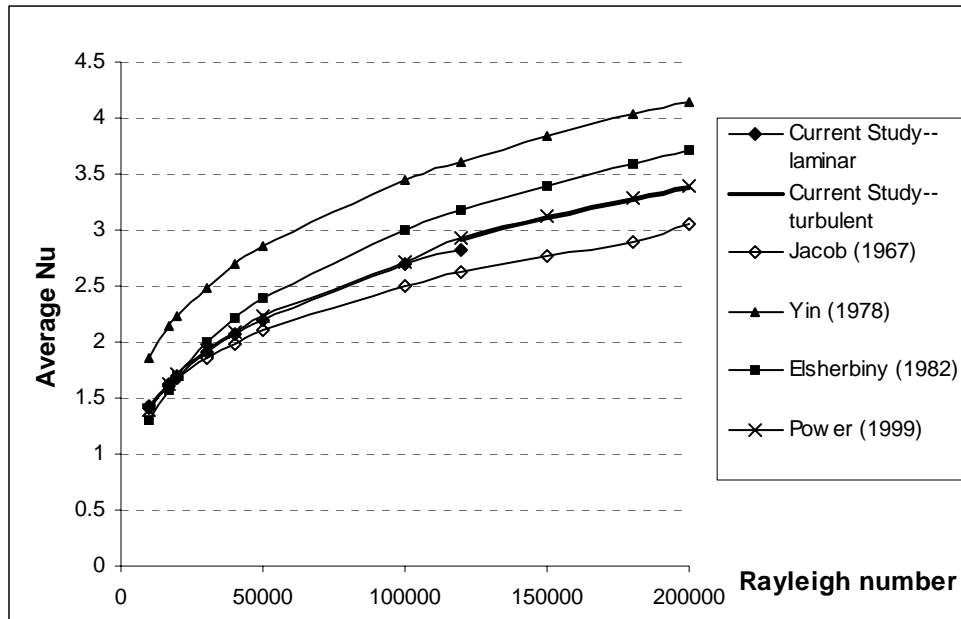


**Figure 8: Average Nu Vs. Ra for  $A=20$**

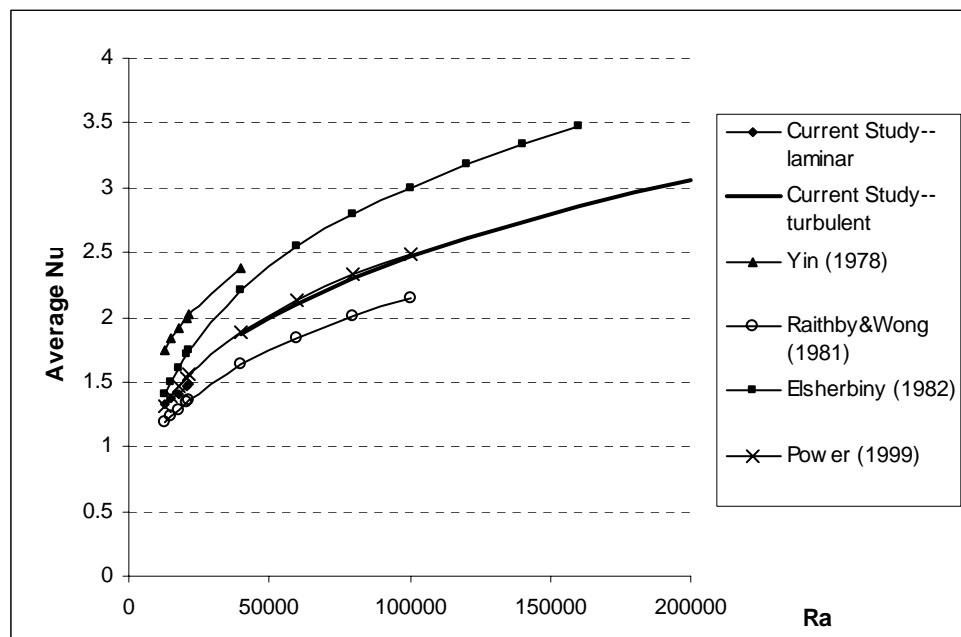


**Figure 9: Average Nu Vs. Ra for  $A=50$**

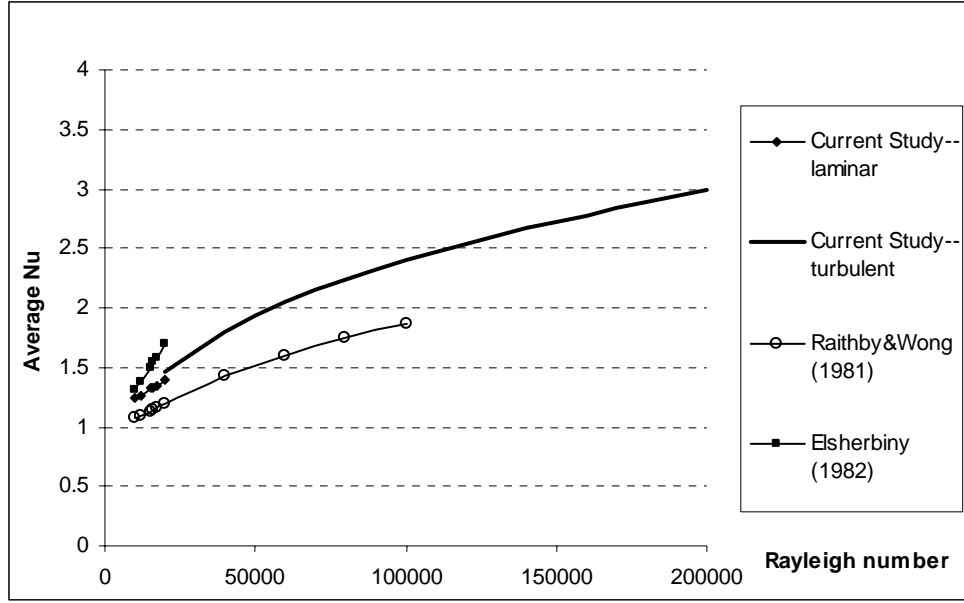


**Figure 10: Average Nu Vs. Ra for A=80**

The relationship of average Nusselt number with respect to Rayleigh number under different aspect ratios are presented in Figures 8, 9 and 10 for  $A=20$ , 50 and 80 respectively. When  $A$  is 20, it can be found that data curve from current numerical simulation lies between the experimental results of Jacob (1967)'s, Yin (1978)'s and Elsherbiny (1982)'s. However, as  $A$  increases, experimental data to be compared with become more and more scarce. Aspect ratio 50 is out of the range of Jacob's correlation. At aspect ratio 80 only Elsherbiny's experimental data is applicable for a small portion of the whole range of Rayleigh number covered in current study. Numerical results from Raithby and Wong (1981) and Power (1999) were also plotted for comparison, for their effective Rayleigh number and aspect ratio range, respectively.

Based on the average Nusselt numbers obtained for all aspect ratios ranging from 20 to 100 and Rayleigh number up to 200,000, a combined correlation of average Nusselt number as a function of aspect ratio and Rayleigh number is developed for turbulent heat transfer in vertical rectangular enclosures, given as below:

$$\text{IN PROGRESS} \quad (20)$$

## 7. Conclusions

IN NEED OF FINAL CORRELATION TO WRAP UP.

## 8. References

Batchelor, G.K., 1954. Heat Transfer by Free Convection Across a Closed Cavity Between Vertical Boundaries at Different Temperatures. *Quarterly of Applied Mathematics*, Vol. 12, pp. 209-223.

Eckert, E.R.G. and Walter O. Carlson. 1961. Natural Convection in an Air Layer Enclosed Between Two Vertical Plates with Different Temperatures. *International Journal of Heat and Mass Transfer*. Vol. 21, pp. 307-315.

Elsherbiny, S.M., G.D. Raithby, K.G.T. Hollands. 1982. Heat Transfer by Natural Convection across Vertical and Incline Air Layers. *Transactions of the ASME*. 96/ Vol. 104, Feb. 1982

FIDAP 8.60 Users and Reference Manual. Fluent Inc., Fluid Dynamics Analysis Package Revision 8.60.

Hinze, J. O., 1959. "Turbulence: An Introduction to Its Mechanism and Theory", McGraw-Hill Book Company, Inc.

Jakob, M. 1967. *Heat Transfer*, Vol. 1, Wiley, New York, 1967, pp. 536-539.

Power, J.P.. 1999. Finite Element Model of Turbulent Flow and Heat Transfer in a Fenestration System. Ph.D. Thesis. Department of Mechanical Engineering, University of Massachusetts.

Raithby, G.D., and Wong, H.H. 1981. Heat Transfer by Natural Convection Across Vertical Air Layers. *Numerical Heat Transfer*. Vol. 4, pp. 447-457.

Yin, S.H., T.Y. Wung and K. Chen. 1978. Natural Convection in an Air Layer Enclosed Within Rectangular Cavities. *International Journal of Heat and Mass Transfer*. Vol. 21, pp. 307-315.

Zhao, Y., 1997. Investigation of Heat Transfer Performance in Fenestration System Based on Finite Element Methods. Ph.D. Thesis, Department of Mechanical and Industrial Engineering, University of Massachusetts.